Available online at www.sciencedirect.com

ScienceDirect

Ceramics International 40 (2014) 1927–1932

CERAMICS INTERNATIONAL

www.elsevier.com/locate/ceramint

Development of highly conductive and transparent copper doped zinc oxide thin films via 2-methoxyethanol modified sol–gel dip-coating technique

Hibah A. Al-Khanbashi[a,*], W. Shirbeeny[a], A.A. Al-Ghamdi[a], Lyudmila M. Bronstein[a,b], Waleed E. Mahmoud[a]

[a]*King Abdulaziz University, Faculty of Science, Physics Department, Jeddah, Saudi Arabia*
[b]*Indiana University, Department of Chemistry, Bloomington, IN 47405, USA*

Received 18 June 2013; received in revised form 17 July 2013; accepted 18 July 2013
Available online 31 July 2013

Abstract

Nanocrystalline copper doped zinc oxide thin films were prepared via a modified 2-methoxyethanol sol–gel dip-coating technique at various concentrations of copper in the range 0–5 wt%. The X-ray diffraction analysis confirmed the copper doped zinc oxide hexagonal wurtzite structure. The copper ions interstitially substitute zinc ions in the hexagonal structure which resulted in the decrease of the crystallite size from 25 nm to 16 nm. A decrease in the lattice parameters was observed up to 2 wt% of copper ions followed by an increase. Scanning electron microscopy showed a homogenous distribution of the prepared films along the glass substrates. Energy dispersive spectroscopy confirmed the stoichiometry and high purity of the prepared films. The optimum optical band gap was achieved at 2 wt% of the copper ion concentration. The prepared films showed a high transparency in the visible region with an average value of 89%. The *I–V* characteristics showed Ohmic behavior up to 3 V. The electrical resistivity showed a lowest value (0.2 Ω cm) for the film doped with 2 wt% of copper.

Keywords: A. Sol–gel; Crystal structure; Dip-coating; Transparency; Resistivity

1. Introduction

Transparent conducting thin films received a great deal of attention because they allow one to achieve large values of electrical conductivity, whilst maintaining high transmission in the visible range of the electromagnetic spectrum [1,2]. Since the advance of this type of materials, vast research and development have gone into commercialization of these thin film coatings [3,4]. The current commercial products are based on n-doped metal oxide thin films, so-called transparent conducting oxides (TCO's). Most of these transparent metal oxides are n-type semiconductors and are employed in various technological applications, such as heat-mirror window-coatings, which control the transmission of infrared energy into and out of buildings, photovoltaic cells, touch-screen technology, and light emitting and plasma screen displays [5–8].

However, p-type transparent metal oxides are nearly non-existent due to difficult fabrication and hole injection into metal oxide semiconductor materials [9,10]. Tin doped indium oxide (ITO) is one of the popular transparent metal oxides that has been widely investigated and used commercially [11]. ITO has electrical conductivity of $\sim 10^4\ \Omega^{-1}\ cm^{-1}$ and transmission of $> 80\%$. This is close to metallic conductivity, in a material that is transparent, thus it has resulted in many important applications such as current spreading layers in light emitting diodes and thermal insulation for windows [12,13]. The high cost of indium and tin, however, has spawned the search for an alternative to ITO and zinc oxide is fast emerging as such.

The unique optoelectronic properties of zinc oxide, the low cost and its nontoxicity have attracted attention in the recent years [14–16]. The electrical and optical properties, high mechanical and chemical stability make zinc oxide the promising material for TCO's. The abundance of ZnO in nature makes it a lower cost material than the majority of the

*Corresponding author. Tel.: +966 544087622.
E-mail address: hibah_alkhanbashi@yahoo.com (H.A. Al-Khanbashi).

0272-8842/$ - see front matter © 2013 Elsevier Ltd and Techna Group S.r.l. All rights reserved.
http://dx.doi.org/10.1016/j.ceramint.2013.07.100

currently used TCO's (SnO_2, ITO). The average amount of zinc available in earth's crust is 132 ppm while for indium, it is only 0.1 ppm and for tin, it is 40 ppm [17].

Herein, we developed a novel procedure to prepare copper doped zinc oxide thin films at different copper concentrations via a modified 2-methoxyethanol sol–gel dip-coating technique to improve the transparency and the conductivity of these films to be close to the ITO values.

2. Experimental

In a typical synthesis, 1 mmol (0.22 g) of zinc acetate $Zn(CH_3COO)_2 \times 2H_2O$ was dissolved in 40 mL of 2-propanol to form a clear zinc acetate solution. Then 1 mmol (0.076 g) of 2-methoxyethanol was added to the zinc acetate solution and kept stirring for 30 min at 60 °C until forming a homogeneous viscous solution. Glass substrates were cleaned by acetone in ultrasonic bath for 2 h, followed by washing with de-ionized water and then dried by nitrogen. The pre-cleaned quartz substrate was immersed into the viscous gel by dipping at cross-head speed 1 mm/min, left in the gel for 5 min and then withdrawn with the same cross-head speed. This process was repeated multiple times until the desired thickness was obtained (220 nm). After the dip coating process the glass coating films were treated at 100 °C for 10 min in an electric oven to evaporate the solvent and to remove organic residues followed by calcination of these films at 350 °C for 2 h.

The zinc hydroxide synthesis was carried out according to the following chemical equation:

$$Zn(CH_3COO)_2(H_2O)_2 + 2C_3H_7OH \rightarrow Zn(OH)_2 + 2C_2H_4O_2 + 2C_2H_5CH_2OH$$

Calcination at 350 °C for 2 h allowed transformation of zinc hydroxide to zinc oxide:

$$Zn(OH)_2 \xrightarrow{350\ ^\circ C (2\ h)} ZnO + H_2O\uparrow$$

Copper doped zinc oxide thin films have been deposited on a glass substrate according to the above procedure with addition of the required amounts of copper nitrate to allow from 1 wt% to 5 wt% of copper. The required amount of copper nitrate was added to the zinc acetate solution, then left stirring until a clear homogeneous viscous solution formation. This viscous solution was served as the coating source.

The X-ray diffraction (XRD) of the films prepared was carried out with Rigaku-Ultima-IV X-ray diffractometer, Seron Inc. Transmission electron microscopy (TEM), selected area electron diffraction (SAED) and energy dispersive X-ray spectroscopy (EDS) were carried out with AIS 2100 TEM microscope at accelerating voltage of 200 kV. The optical measurements were conducted with WVASE32 ellipsometry supplied by J.A. Woollam Co., Inc. and the electrical measurements were performed with the Keithley 6514 electrometer.

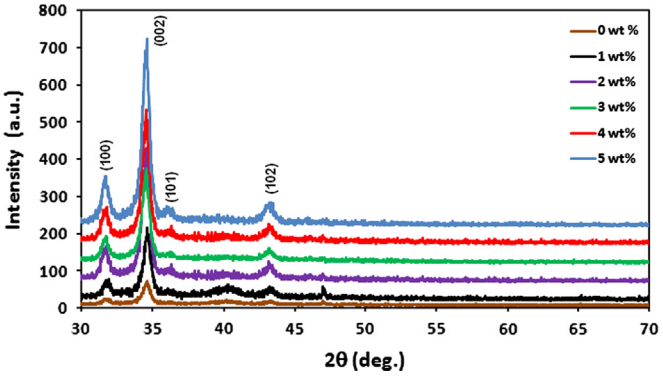

Fig. 1. XRD patterns for copper doped zinc oxide thin films.

3. Results and discussion

3.1. X-ray diffraction analysis of copper doped zinc oxide thin films

Fig. 1 depicts a typical X-ray diffraction patterns for the Cu-doped with ZnO thin films at different dopant concentrations. The diffraction peaks at the angles 31.4°, 34.53°, 36.5° and 43.2° are assigned to the reflections from the (100), (002), (101) and (102) planes, respectively. All the patterns are assigned to the hexagonal zinc oxide structure according to ASTM data card 5-664 [18]. No phase corresponding to copper or copper oxide was detected in the XRD patterns. According to the results obtained from XRD measurements one can conclude that the zinc oxide hexagonal structure is preserved up to 5 wt% of the copper dopant. The preferential orientation is along the (002) crystal plane at $2\theta = 34.53^\circ$ for all prepared films. The diffraction peak (002) is also slightly shifted as the Cu-dopant concentration increased. This resulted in a change in the lattice constants. In order to calculate the lattice constant parameters, the Bond Model was utilized [19]. According to Bragg's law, the inter-space lattice parameter, d_{hkl}, can be estimated from the diffraction angle as follows

$$\lambda = 2d_{hkl} \sin\ \theta \quad (1)$$

where λ is the wavelength of the X-ray source and d_{hkl} is the lattice spacing parameter.

Eq. (1) may be written in the form

$$\frac{1}{d^2{}_{hkl}} = \frac{4}{\lambda^2} \sin^2\theta \quad (2)$$

For hexagonal crystal structure, the lattice constants, a and c, may be given as

$$\frac{1}{d_{hkl}{}^2} = \frac{4(h^2 + hk + k^2)}{3a^2} + \frac{l^2}{c^2} \quad (3)$$

Combining (2) with (3), one obtains

$$\sin^2\theta = \left[\frac{\lambda^2}{3a^2}(h^2 + hk + k^2)\right] + \left[\frac{\lambda^2}{4c^2}l^2\right] \quad (4)$$

The a and c lattice constants for the copper doped zinc oxide hexagonal structure was estimated according to Eq. (4) and presented in Fig. 2.

Fig. 2 reveals the variation of lattice parameters against the copper ion concentration. The lattice constants first decreased as the Cu dopant concentration increased up to 2 wt% then increased. One can assume that an interstitial substitution of Cu in Zn sites has occurred up to 2 wt% and resulted in a reduction of the d-spacing of the ZnO hexagonal structure. At higher Cu concentrations, the copper ions are apparently located between the ZnO planes, causing an increase in the d-spacing [20].

The average crystallite sizes in the copper doped zinc oxide thin films were determined by Scherrer's formula [21]

$$R = \frac{k\,\lambda}{\beta \cos\,\theta} \tag{5}$$

where R is the domain crystallite size, λ is the wavelength of X-ray source, k is the constant which is equal 0.94 for hexagonal structure, β is the full width at half maximum and θ is the diffraction angle. The average crystalline sizes of the copper doped zinc oxides are presented in Table 1.

3.2. Surface morphology of Cu-doped zinc oxide thin films

The surface morphology of the films on a glass substrate was investigated by the scanning electron microscopy using the sample containing 1 wt% of Cu as an example. Fig. 3 displays the SEM image for the surface of the as deposited Cu-doped zinc oxide film. The surface of the film contains grains with an average size of 162 ± 11 nm. These grains are homogenously distributed along the surface of the films showing no voids.

The elemental composition of the Cu-doped zinc oxide film with 1 wt% of Cu was estimated by EDS (Fig. 4). The EDS spectrum shows that the sample contains only copper, zinc and oxygen. No other elements were found confirming the high purity of the films prepared. The molar ratios of the Cu:Zn:O are indicated in the table inset of Fig. 4 which correspond to 1.01 wt% Cu, 47.16 wt% Zn, and 51.83 wt% of oxygen, confirming the expected stoichiometry of the film.

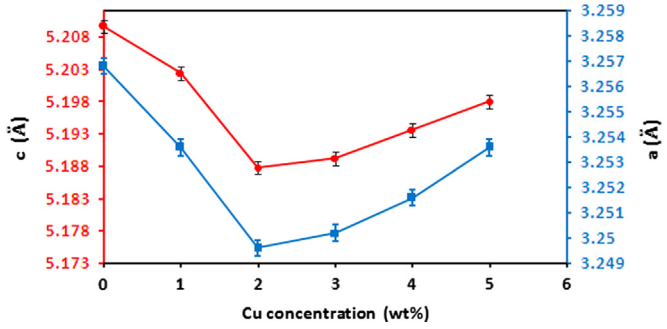

Fig. 2. Calculated lattice constants for Cu-doped zinc oxide thin films.

3.3. Optical properties of copper doped zinc oxide thin films

The optical absorption spectra of the as-prepared films were examined to estimate the optical band energy gap, E_g, according to Tauc's relation [22]

$$\alpha = \frac{A}{h\nu}(h\nu - E_g)^n \tag{6}$$

where α is the absorption coefficient ($\alpha = 4\pi k/\lambda$), $h\nu$ is the incident photon energy and n is the constant, the value of which depends on the transition type. For allowed direct

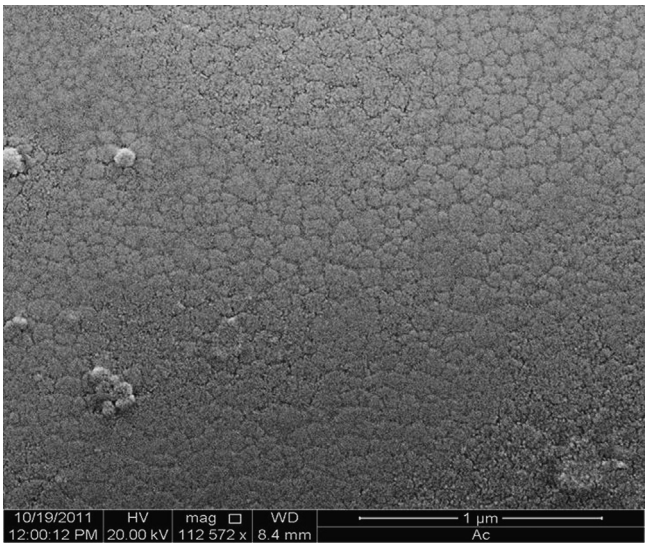

Fig. 3. SEM image for the surface of the $Zn_{0.99}Cu_{0.01}O$ thin film.

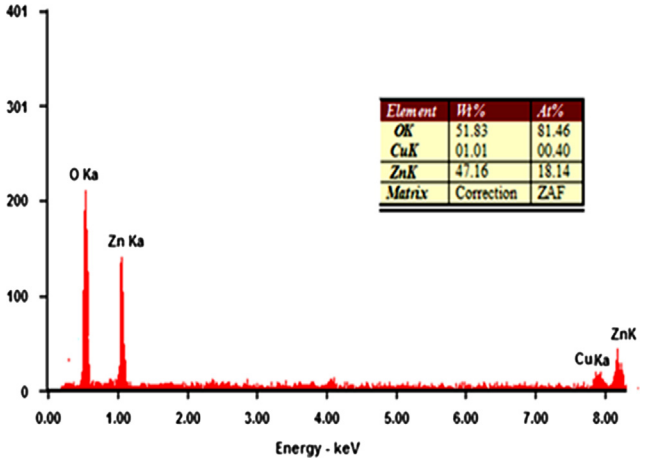

Fig. 4. EDS spectrum of the $Zn_{0.99}Cu_{0.01}O$ thin film.

Table 1
Average domain crystalline size of Cu-doped zincr oxide films.

Cu amount (wt%)	0	1	2	3	4	5
R (nm)	25 ± 3	18 ± 2	9 ± 1	11 ± 1	13 ± 2	16 ± 1

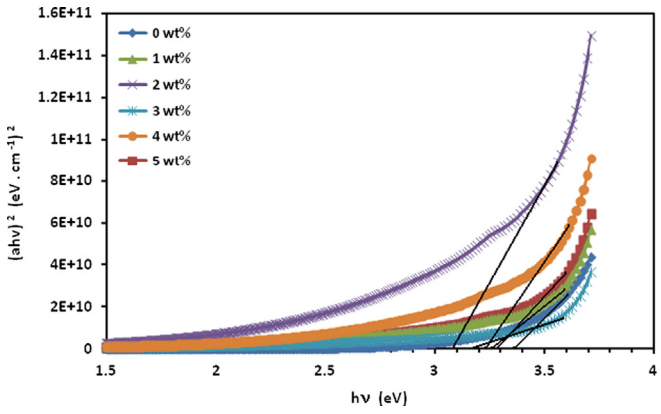

Fig. 5. The dependence of $(\alpha h\nu)^2$ on the $(h\nu)$ for Cu-doped zinc oxide thin films.

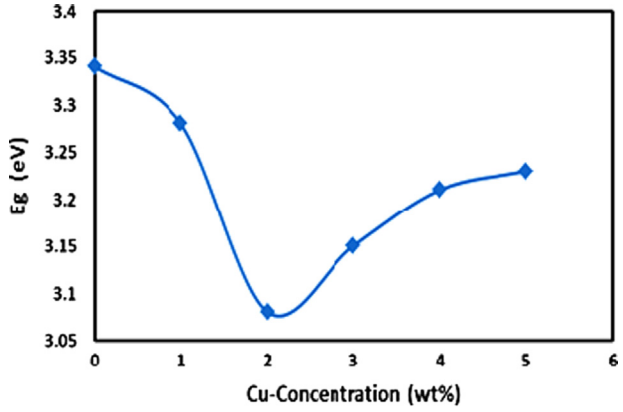

Fig. 6. The variation of E_g with copper concentration for Cu-doped zinc oxide thin films.

transitions the following equation is true:

$$(\alpha h\nu)^2 = A\,(h\nu - E_g) \tag{7}$$

Fig. 5 exhibits the dependence of $(\alpha h\nu)^2$ on the $h\nu$. The optical band gap was estimated from this figure for all deposited films. Fig. 6 shows the influence of the copper concentration on the optical band energy gap of the ZnO thin films. One can see that the band energy gap decreased with increasing concentration up to 2 wt% and then increased. This behavior may be attributed to the Moss–Burstein effect. For the Cu concentration above 2 wt%, the copper ions tend to locate between ZnO lattice planes which results in an increase of the hopping path of charge carriers and in turn, an increase of the band gap [23].

The optical transmittance is an essential optical parameter for transparent metal oxides. The transmittance was determined from the optical absorption coefficient according to $(T = e^{-\alpha d})$, where d is the film thickness which is determined from ellipsometry measurements ($\approx 214 \pm 6$ nm). The transmittance as a function of a wavelength was plotted in Figs. 7 and 8 for Cu-doped zinc oxide thin films. Clearly, the optical transmittance is decreased with the addition of the Cu ions with the lowest value of 80% at 3 wt% of copper. At lower and higher copper concentrations, the transmittance is higher, indicating that the film transparency is largely preserved.

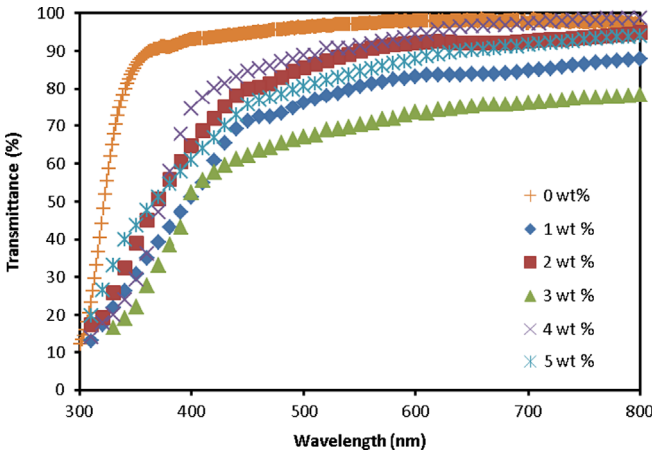

Fig. 7. The optical transmittance against wavelength for Cu-doped zinc oxide films.

3.4. Electrical properties of copper doped zinc oxide thin films

Fig. 9 shows the *I–V* characteristic curves for the ZnO thin films prepared at different concentrations of copper ions. One can see that the samples exhibit a linear relationship up to 3 V, which is assigned to Ohmic behavior. The *I–V* relation is mainly defined by the well known relation $I \propto V^n$ [24], where n is an exponent, the value of which determines the kind of the conduction mechanism. For $n = 1$, the conduction mechanism obeys Ohm's law, while for $n = 2$, the conduction mechanism is a space charge limited conduction mechanism (SCLCM) [25]. The value of n can be obtained from the slope of log I vs. log V. For all prepared samples it was found that the value of $n \approx 1$, confirming that the films follow Ohmic behavior. It was also observed that at a fixed voltage, the current depends on the amount of copper ions incorporated in the zinc oxide structure.

The resistivity of the samples was also measured. Fig. 10 shows the evolution of the electrical resistivity of ZnO thin films as a function of Cu concentration. The electrical resistivity decreased with increasing copper concentration, reaching the minimum value at the copper content of 2 wt%. However, upon the further increase of the copper concentration, the resistivity values increase. For the Cu content below 2 wt% the decrease of resistivity can be due to the increase of the amount of Cu atoms that are incorporated into the ZnO lattice in the Zn sites, supplying a hole for each Cu atom, until maximum solubility of Cu in the ZnO lattice is reached, matching minimum value of resistivity. This means the Cu ions in the ZnO lattice act as acceptor impurities. For the Cu content above 2 wt%, the copper ions are no longer able to occupy more Zn sites and a segregation of Cu ions takes place around the grain boundaries or interstices, causing a rise of the electrical resistivity.

4. Conclusion

Copper doped ZnO oxide thin films of different compositions have been successfully prepared via a modified 2-methoxyethanol

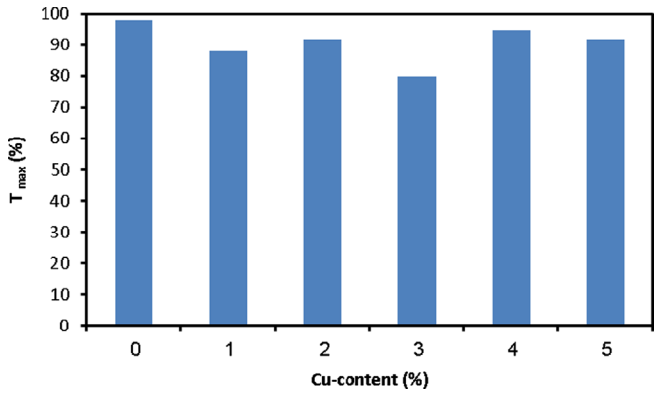

Fig. 8. The maximum transmittance against copper concentration in Cu-doped zinc oxide films.

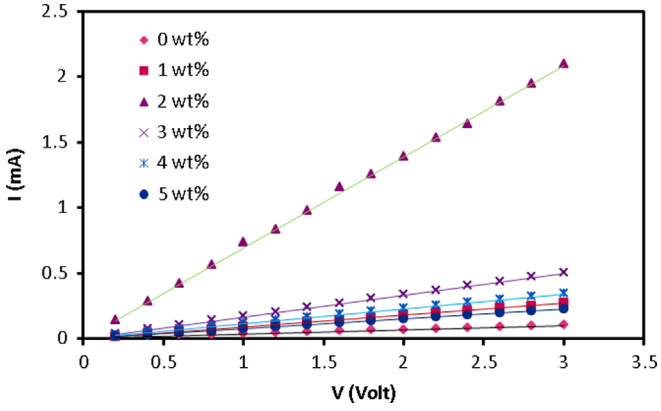

Fig. 9. *I–V* characteristic curves for Cu-doped zinc oxide thin films.

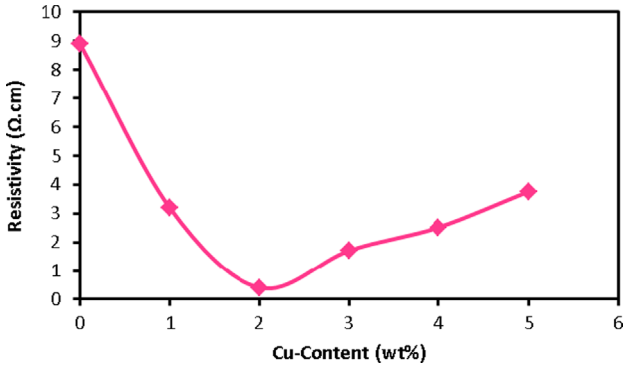

Fig. 10. Resistivity dependence on the Cu concentration for Cu-doped zinc oxide thin films.

sol–gel dip-coating technique. The films are homogeneous with evenly distributed grains on the surface of a glass substrate. XRD indicates that the ZnO hexagonal phase structure has been preserved after incorporation of copper ions in the range 1–5 wt % but the lattice constants are copper ion concentration dependent. The copper ions interstitially substitute zinc ions in the hexagonal structure which results in a decrease of the crystal size from 25 nm to 16 nm. EDS confirmed the high purity of the prepared films and intended stoichiometry. The films prepared attained a lowest optical band gap at 2 wt% of copper. The electrical measurements depicted a linear regression up to 3 V. The lowest electrical resistivity was also achieved at 2 wt.% of the copper ion concentration.

References

[1] K.L. Chopra, S. Major, D.K. Pandya, Transparent conductors A status review, Thin Solid Films 102 (1983) 1–46.
[2] P.P. Edwards, A. Porch, M.O. Jones, D.V. Morgan, R.M. Perks, Basic materials physics of transparent conducting oxides, DaltonTransactions 19 (2004) 2995–3002.
[3] H. Kawazoe, K. Ueda, Transparent conducting oxides based on the spinel structure, Journal of the American Ceramic Society 82 (1999) 3330–3336.
[4] Z.M. Jarzebski, Preparation and physical properties of transparent conducting oxide films, Physica Status Solidi 71 (1982) 13–41.
[5] U.S. Joshi, Y. Matsumoto, K. Itaka, M. Sumiya, H. Koinuma, Combinatorial synthesis of Li-doped NiO thin films and their transparent conducting properties, Applied Surface Science 252 (2006) 2524–2528.
[6] C.H. Lau, L. Zhuang, K.H. Wong, In-doped transparent and conducting cubic magnesium zinc oxide thin films grown by pulsed laser deposition, Physica Status Solidi B 244 (2007) 1533–1537.
[7] K. Ellmer, G. Vollweiler, Electrical transport parameters of heavily-doped zinc oxide and zinc magnesium oxide single and multilayer films heteroepitaxially grown on oxide single crystals, Thin Solid Films 496 (2006) 104–111.
[8] B.J. Ingram, M.I. Bertoni, K.R. Poeppelmeier, K.R. Mason, Point defects and transport mechanisms in transparent conducting oxides of intermediate conductivity, Thin Solid Films 486 (2005) 86–93.
[9] E. Arca, K. Fleischer, I.V. Shvets, Magnesium, nitrogen codoped Cr_2O_3: A p-type transparent conducting oxide, Applied Physics Letters 99 (2011) 111910.
[10] S. Götzendörfer, P. Löbmann, Influence of single layer thickness on the performance of undoped and Mg-doped $CuCrO_2$ thin films by sol–gel processing, Journal of Sol–Gel Science and Technology 57 (2011) 157–163.
[11] T. Minami, Present status of transparent conducting oxide thin-film development for Indium-Tin-Oxide (ITO) substitutes, Thin Solid Films 516 (2008) 5822–5828.
[12] S. Laux, N. Kaiser, A. Zöller, R. Götzelmann, H. Lauth, H. Bernitzki, Room-temperature deposition of indium tin oxide thin films with plasma ion-assisted evaporation, Thin Solid Films 335 (1998) 1–5.
[13] D.C. Paine, T. Whitson, D. Janiac, R. Beresford, C.O. Yang, B. Lewis, A study of low temperature crystallization of amorphous thin film indium-tin-oxide, Journal of Applied Physics 85 (1999) 8445–8450.
[14] W.E. Mahmoud, A.M. Al-Sanoosi, Synthesis, characterization and photoluminescence of ZnO:Cd rosette-like nanostructures using solution process, Superlattices and Microstructures 51 (4) (2012) 506–511.
[15] W.E. Mahmoud, A.A. Al-Ghamdi, S. Al-Heniti, S. Al-Ameer, The influence of temperature on the structure of Cd-doped ZnO nanopowders, Journal of Alloys and Compounds 491 (1–2) (2010) 742–746.
[16] W.E. Mahmoud, A.A. Al-Ghamdi, Synthesis of CdZnO thin film as a potential candidate for optical switches, Optics and Laser Technology 42 (7) (2010) 1134–1138.
[17] H.L. Hartnagel, Semiconducting transparent thin films, Institute of Physics Publishing, Bristol, UK, 1995 (ISBN 978–0750303224).
[18] W.E. Mahmoud, Synthesis and optical properties of Ce-doped ZnO hexagonal nanoplatelets, Journal of Crystal Growth 312 (21) (2010) 3075–3079.
[19] S.A. Al-Ghamdi, S.H. Al-Heniti, W.E. Mahmoud, Schottky barrier effect of ZnO modified methyl glycol thin films for detection of hydrogen sulfide gas, Ceramics International 39 (5) (2013) 5015–5030.

[20] W.E. Mahmoud, T. Al-Harbi, Synthesis, characterization and photoluminescence properties of Sn doped ZnO nanonails, Journal of Crystal Growth 327 (1) (2011) 52–56.
[21] W.E. Mahmoud, A novel photodiode made of hybrid organic/inorganic nanocomposite, Journal of Physics D Applied Physics 42 (2009) 15 (Art. no. 155502).
[22] A.A. Al-Ghamdi, W.E. Mahmoud, S.J. Yaghmour, F.M. Al-Marzouki, Structure and optical properties of nanocrystalline NiO thin film synthesized by sol–gel spin-coating method, Journal of Alloys and Compounds 486 (1–2) (2009) 9–13.
[23] W.E. Mahmoud, F. Al-Marzouki, S. Al-Ameer, F. Al-Hazmi, Synthesis and characterization of one-dimensional vertically aligned Sb-doped ZnO nanowires, Journal of Applied Crystallography 45 (2) (2012) 182–185.
[24] W.E. Mahmoud, A.A. Al-Ghamdi, F. El-Tantawy, S. Al-Heniti, Synthesis, characterization and charge transport mechanism of CdZnO nanorods, Journal of Alloys and Compounds 485 (1–2) (2009) 59–63.
[25] M. Hafez, F. Al-Marzouki, W.E. Mahmoud, Single crystalline quasi aligned one dimensional P-type Cu_2O nanowire for improving Schottky barrier characteristics, Materials Letters 65 (12) (2011) 1868–1870.